IEEE Photonics Journal
An IEEE Photonics Society Publication

Open Access

Experimental Investigation on Low-Complexity Adaptive Equalizer Including RSOP Tracking and Phase Recovery for 112 Gb/s PDM-QPSK Transmission System

Volume 13, Number 2, April 2021

Pin Yi
Di Li
Haiping Song
Mengfan Cheng
Deming Liu
Lei Deng

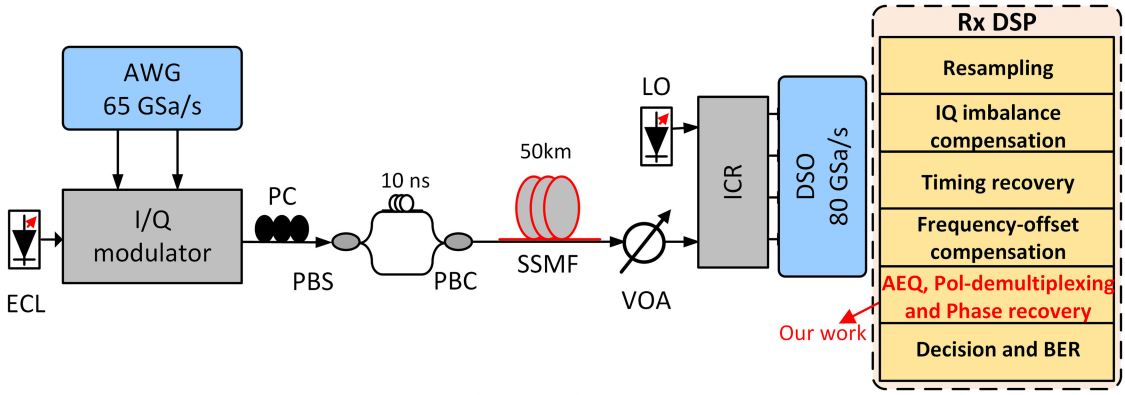

The experimental setup of 112 Gb/s PDM-QPSK coherent optical transmission system using the proposed schemes

DOI: 10.1109/JPHOT.2021.3062727

Experimental Investigation on Low-Complexity Adaptive Equalizer Including RSOP Tracking and Phase Recovery for 112 Gb/s PDM-QPSK Transmission System

Pin Yi, Di Li, Haiping Song, Mengfan Cheng, Deming Liu, and Lei Deng

Wuhan National Laboratory for Optoelectronics (WNLO) and School of Optical and Electronic Information, Huazhong University of Science and Technology, Wuhan 430074, China

DOI:10.1109/JPHOT.2021.3062727

Manuscript received January 3, 2021; revised February 21, 2021; accepted February 25, 2021. Date of publication March 1, 2021; date of current version March 18, 2021. This work was supported in part by the National Key Research and Development Program of China under Grant 2018YFB1800903, in part by the National Natural Science Foundation of China under Grant 61675083, in part by the Fundamental Research Funds for Central Universities HUST under Grant 2019kfyXMBZ033, and in part by the State Key Laboratory of Advanced Optical Communication Systems Networks, China under Grant 2019GZKF7. Corresponding author: Lei Deng (e-mail: denglei_hust@mail.hust.edu.cn).

Abstract: A low-complexity adaptive equalizer including equalization, rotation of state of polarization (RSOP) tracking, and phase recovery is proposed for coherent optical polarization-division-multiplexing (PDM) quadrature phase-shifting keying (QPSK) transmission system. A conventional N-tap 2 $\times$ 2 butterfly finite impulse response filter is simplified to two N-tap filters and a 1-tap 2 $\times$ 2 filter. Two N-tap filters could compensate for inter-symbol interference and residual chromatic dispersion based on the same error cost function from the power sum of two polarization coupling constant modulus signals. 1-tap 2 $\times$ 2 filter which works on the nonlinear principal component analysis (NPCA) criterion is designed for joint polarization demultiplexing and phase recovery. NPCA is proved to not only void the singularity problem in the constant modulus algorithm (CMA) but also has faster tracking capability. Two kinds of adaptive equalizers using least mean squares NPCA (LMS-NPCA) and recursive least squares NPCA (RLS-NPCA) are compared in our simulation and experiment. In an experiment of 112 Gb/s PDM-QPSK transmission over 50 km standard single-mode fiber, the proposed two schemes have better transmission performance at RSOP speed of 1 Mrad/s and 5 Mrad/s compared to the conventional CMA and Viterbi-Viterbi phase estimation (VVPE) scheme. The reduced complexity of the proposed schemes is more than 40%.

Index Terms: Digital coherent communication, adaptive equalization (AEQ), nonlinear principal component analysis (NPCA), polarization de-multiplexing, phase recovery, rotation of state of polarization (RSOP).

1. Introduction

With the rapidly widespread popularity of 5th generation mobile communication, cloud services, and high-definition video streaming, medium and short-reach optical networks such as mobile fronthaul, datacenter interconnects (DCI), and passive optical network (PON) are facing an urgent requirement in traffic capability. Generally, the intensity modulation and direct detection (IM/DD) technique is preferred because of its characteristics of low cost and low complexity [1]–[3]. As further increasing the channel capacity, the coherent detection scheme with digital signal processing (DSP) is now being a promising candidate to meet these demands due to its higher receiver sensitivity and spectrum efficiency [4]. However, computational complexity and power consumption of DSP algorithms in coherent detection are the most major concern for medium and short-reach applications. Furthermore, a polarization division multiplexing (PDM) coherent optical transmission system is usually limited by the ultrafast rotation of state of polarization (RSOP) [5], [6] and the time-varying laser phase noise. Therefore, a low-complexity and high-performance DSP algorithm is highly desired.

In a conventional coherent DSP flow, the time-domain adaptive equalization (AEQ) algorithm based on the N-tap 2×2 butterfly finite impulse response (FIR) filter occupies a large portion of the overall DSP complexity [7]. To reduce this computational complexity, several modified algorithms have been proposed recently [8], [9]. A frequency-domain fixed dispersion compensation equalizer for static chromatic dispersion (CD) can be applied before a time-domain AEQ [8], which can reduce the required number of time-domain FIR filter taps. However, the overall complexity is increased due to the digital transformation operation between the frequency domain and time domain. In [9], a frequency-domain AEQ is proposed to get a lower complexity than the time-domain AEQ when the fiber distance is long. But it will get a little higher complexity when the number of FIR taps is relatively few. Modern fibers have very small polarization mode dispersion (PMD) parameters ($<$0.1 ps/km$^{1/2}$) [10], and thus two kinds of similar simplified time-domain AEQs have also been reported in [11], [12]. K. Matsuda has proposed a simplified AEQ constituted with a 1-tap butterfly FIR filter for polarization de-multiplexing and two N-tap FIR filters for adaptive equalization, and PMD compensation is neglected (hereinafter referred to $1-$N structure) [11]. X. Zhang has proposed another kind of cascade scheme in reverse order in which the first section consists of two N-tap FIR filters and the second section is a 1-tap butterfly FIR filter (hereinafter referred to N-1 structure) [12]. Compared to the conventional AEQ, the complexity of these two algorithms are both reduced by about 40% without loss of equalization performances. Compared to the $1-$N structure, adaptive equalization in the N-1 structure works polarization-independently before polarization de-multiplexing for reducing the impact of fiber dispersion on the error cost function convergence [12], [13]. Moreover, the constant modulus algorithm (CMA) is both used in these two simplified AEQs for polarization de-multiplexing, resulting in the singularity problem in some scenarios [14].

Apart from the algorithm complexity, the dynamic polarization tracking capability of DSP algorithms also becomes critical in real application scenarios. Some extreme environments like the lightning strike will not only make direct striking vibration on the optical ground wire cable (OPGW) which will generate a polarization state change but also induce the Kerr effect and Faraday effect which induce ultra-fast RSOP [15]. In Europe, there are about 30 direct lightning strikes per 100 km of OPGW per year [6]. It has been reported that this kind of fast polarization rotation will be as fast as 5.4 Mrad/s [5], and this will cause the commonly used polarization tracking algorithms such as CMA invalidation. To address this issue, several fast polarization tracking algorithms including Kalman filter (KF) [16], independent component analysis (ICA) [17], and nonlinear principal component analysis (NPCA) [18], [19] have been proposed recently. KF is a widely used dynamic tracking technology, and it can track RSOP quickly by constructing a measurement equation and process equation suitable for the received PDM signals. ICA and NPCA are both blind source separation technologies. They are widely used for the signal separation to estimate N-dimensional de-mixed unitary matrix based on the minimization of high-order statistics, which can effectively void the singularity problem. In ICA, a nonlinear active function is employed to approximate the

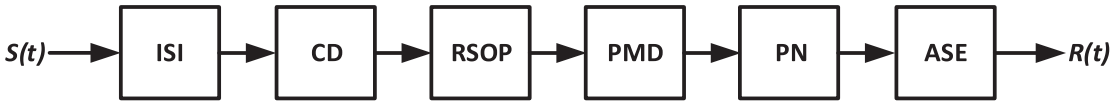

Fig. 1. The transmission model of a typical coherent optical PDM transmission system.

probability density function (PDF) of signals, but it is difficult to obtain the true PDF especially when the scenario of high polarization rotation rate is considered. NPCA does not need to construct the PDF of signal, and only a particular form of the nonlinear function is used [19]. However, all the above polarization tracking algorithms cannot compensate for the inter symbol interference (ISI) and residual chromatic dispersion in real transmission systems. Therefore, adaptive multi-tap FIR filters are essential. Besides, carrier phase recovery is another important part of the conventional coherent DSP algorithm. Conventional solutions such as Viterbi-Viterbi phase estimation (VVPE) [20] and blind phase search (BPS) algorithm [21] are both individual modules for phase recovery. Thanks to the fact that NPCA can separate independent in-phase and quadrature components of complex signals, no additional conventional phase recovery scheme is required when NPCA is used for RSOP tracking.

In this paper, we have proposed a low-complexity adaptive equalizer including fast RSOP tracking and phase recovery for a high-speed PDM optical transmission system. The proposed algorithm includes two N-tap one-dimensional polarization-independent FIR filters for adaptive channel estimation and a 2 $\times$ 2 butterfly filter based on NPCA for joint dynamic RSOP tracking and phase recovery. The conventional algorithm using CMA and VVPE, the proposed algorithm using least mean squares NPCA (LMS-NPCA), and the proposed algorithm using recursive least squares NPCA (RLS-NPCA) are all analyzed and compared. The results show that compared to the conventional scheme, the proposed two algorithms show the stronger capability to track RSOP and lower computational complexity. To be specific, in an experiment of 112 Gb/s PDM-QPSK signal transmission over 50km SSMF, the proposed two schemes have better bit error rate (BER) performance at the RSOP speed of 1 Mrad/s and 5 Mrad/s compared to the conventional scheme. And the reduced computational complexity by using these two schemes is more than 40%.

2. Principle

There are lots of impairments that existed in a typical coherent optical PDM transmission system, such as ISI induced by bandwidth-limited devices, CD, RSOP, PMD, phase noise (PN), and amplified spontaneous emission noise (ASE). A convolution coupled transmission model for an optical PDM transmission system could be described as

$$R(t) = H(t) \otimes S(t) = \begin{bmatrix} h_{xx}(t) & h_{xy}(t) \\ h_{yx}(t) & h_{yy}(t) \end{bmatrix} \otimes S(t) + n(t), \tag{1}$$

where $\otimes$ represents the convolution operation. Two-dimensional vector $S(t)$ and $R(t)$ denote transmitted and received signals, respectively. $H(t)$ represents the transmission matrix of this optical transmission system, and $n(t)$ describes the additive white Gaussian noise. To further analyze the impact of different impairments on the whole transmission matrix, a typical optical PDM transmission system is modeled as Fig. 1, and thus the transmission matrix $H(t)$ in (1) can be expressed as [22]

$$H(t) = \begin{bmatrix} h_{xx}(t) & h_{xy}(t) \\ h_{yx}(t) & h_{yy}(t) \end{bmatrix} = e^{j(\triangle\omega t + \theta(t))} \begin{bmatrix} h_x(t) & 0 \\ 0 & h_y(t) \end{bmatrix}_{CD+ISI} \otimes \begin{bmatrix} p_{xx}(t) & p_{xy}(t) \\ p_{yx}(t) & p_{yy}(t) \end{bmatrix}_{PMD} \otimes \begin{bmatrix} j_{xx}(t) & j_{xy}(t) \\ j_{yx}(t) & j_{yy}(t) \end{bmatrix}_{RSOP}, \tag{2}$$

where $\triangle\omega$ denotes the frequency offset between the laser source and the local oscillator, and $\theta(t)$ denotes the time-varying phase noise. $h(t)$ represents the polarization-independent dispersion effects including CD and ISI, $p(t)$ describes PMD, and $j(t)$ denotes the coupling coefficient of

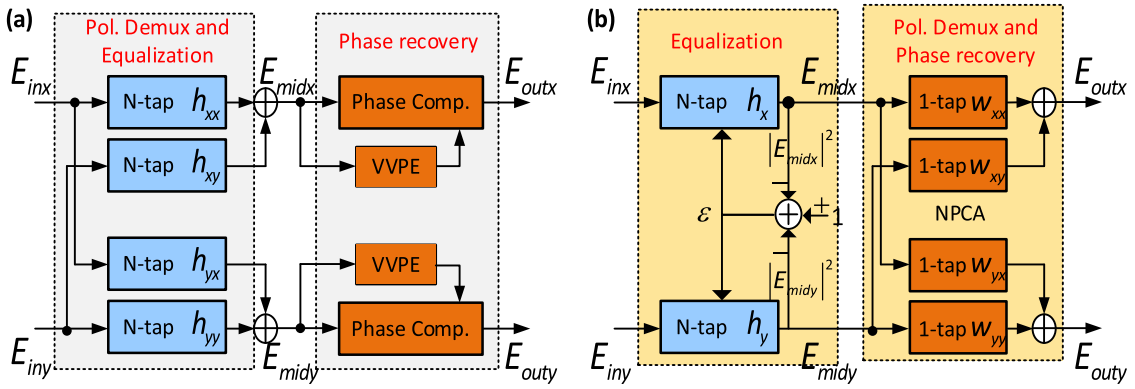

Fig. 2. The structure of the conventional CMA+VVPE algorithm (a) and the proposed adaptive equalizer (b).

RSOP. Because modern fibers have a very small PMD parameter ($<$0.1 ps/km$^{1/2}$), the accumulated difference group delay in two orthogonal polarization signals is much less than single symbol duration for medium and short-reach optical networks [13]. Therefore, a simplified transmission model could be constructed as

$$R(t) = \begin{bmatrix} h_x(t) & 0 \\ 0 & h_y(t) \end{bmatrix}_{CD+ISI} \otimes \begin{bmatrix} j_{xx}(t) & j_{xy}(t) \\ j_{yx}(t) & j_{yy}(t) \end{bmatrix}_{RSOP} \cdot e^{j(\Delta\omega t+\theta(t))} \cdot S(t) + n(t). \tag{3}$$

Note that RSOP will lead to an instantaneous mixing of two orthogonal polarization signals, the convolution operation of the RSOP coupling matrix and $S(t)$ can be converted to the multiplication operation. To compensate for these impairments, a conventional multiple-input and multiple-output (MIMO) equalizer structure in [7] can be simplified by separating the operation of polarization-independent dispersion equalization and polarization de-multiplexing based on (3). Moreover, for ultra-fast RSOP tracking, NPCA is introduced in our scheme as a joint polarization de-multiplexing and phase recovery scheme after adaptive equalization.

Based on the transmission model described in (3), a novel adaptive equalizer is proposed in Fig. 2(b). The first part is two N-tap polarization-independent FIR filters based on constant modulus signals for adaptive equalization, and the second part is a 1-tap 2 $\times$ 2 butterfly filter based on NPCA for joint polarization de-multiplexing and phase recovery. Compare to the conventional N-tap 2 $\times$ 2 butterfly CMA filter and VVPE in Fig. 2(a), two inessential sets of cross taps and an additional conventional phase recovery module based on VVPE are omitted in the proposed scheme.

In the proposed scheme, the input signals first enter two independent N-tap FIR filters. Assuming these two FIR filters have already converged to an ideal state, all dispersion effect and frequency offset have been compensated, and thus two output polarization signals can be expressed as

$$\begin{bmatrix} E_{midx} \\ E_{midy} \end{bmatrix} = e^{j(\theta(t))} \begin{bmatrix} j_{xx}(t) & j_{xy}(t) \\ j_{yx}(t) & j_{yy}(t) \end{bmatrix} \cdot \begin{bmatrix} S_x \\ S_y \end{bmatrix} = e^{j(\theta(t))} \cdot J(t) \cdot \begin{bmatrix} S_x \\ S_y \end{bmatrix}, \tag{4}$$

where S_x/S_y denote the transmitted two polarization signals, $J(t)$ is a unitary Jones matrix [7], and E_{midx}/E_{midy} are the output signals of two independent FIR filters. Furtherly, we can find that

$$|E_{midx}|^2 + |E_{midy}|^2 = J(t) \cdot J(t)^H \cdot (|S_x|^2 + |S_y|^2) = (|S_x|^2 + |S_y|^2) = \text{constant}, \tag{5}$$

where H denotes the Hermitian transposition. It could be observed that the output signals E_{midx}/E_{midy} have not been de-multiplexed, and thus it cannot meet the CMA condition. The reason is that the received signal influenced by RSOP is exactly the projection of the transmitted two orthogonal polarization signals with rotation. Therefore, for QPSK signals the power sum of optical signals in two orthogonal polarization states remain constant. In this case, the conventional CMA error cost

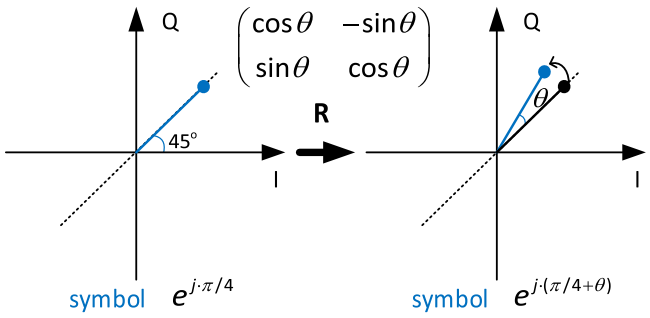

Fig. 3. The phase noise model in the coherent optical PDM transmission system.

function [14] could be modified by

$$\text{Error} = \text{constant} - (|E_{midx}|^2 + |E_{midy}|^2). \tag{6}$$

Based on the above analysis, the equalization and the coefficient update process could be expressed as

$$E_{midx} = \sum_{i=1}^{N} h_x(i) \cdot E_{inx}(i), \tag{7}$$

$$E_{midy} = \sum_{i=1}^{N} h_y(i) \cdot E_{iny}(i), \tag{8}$$

$$h_x = h_x + \mu\varepsilon E_{midx}[E_{inx}]^H, \tag{9}$$

$$h_y = h_y + \mu\varepsilon E_{midy}[E_{iny}]^H, \tag{10}$$

$$\varepsilon = 1 - (|E_{midx}|^2 + |E_{midy}|^2), \tag{11}$$

where μ denotes the step size of the equalization operation, $[E_{inx}]/[E_{iny}]$ represents an N-dimensional received signals vector, and h_x/h_y are the tap coefficients of FIR filters. For convenience, the above algorithm is called the modified CMA (M-CMA) and the conventional CMA algorithm is called C-CMA. The proposed structure which consists of two N-tap FIR filters and a 1-tap butterfly FIR filter is hereinafter referred to N-1 structure. The first two polarization-independent N-tap FIR filters not only compensate for the fiber dispersion and ISI but also makes two output signals orthogonal, and this could effectively improve the subsequent polarization de-multiplexing performance compared to the $1 - N$ structure in [11]. CD and ISI will influence the optimal convergence performance of the 1-tap 2×2 butterfly polarization de-multiplexing filter, so fiber dispersion should be compensated before the polarization de-multiplexing.

After equalization, a 2×2 filter based on NPCA is used to realize joint polarization de-multiplexing and phase recovery as mentioned above. According to (4), the equalized signals are still impaired by RSOP and phase noise. As explained in literature [23], the RSOP model can be expressed by a unitary Jones transformation matrix J, which can be mathematically given as

$$J = \begin{bmatrix} j_{xx} & j_{xy} \\ j_{yx} & j_{yy} \end{bmatrix} = \begin{bmatrix} a + jb & c + jd \\ -c + jd & a - jb \end{bmatrix}, \tag{12}$$

where $a^2 + b^2 + c^2 + d^2 = 1$, only 3 parameters are independent. The phase noise can be modeled as a rotation transformation of standard constellation symbols.

According to a visual representation in Fig. 3, the impairment from the phase noise can be described as

$$\begin{pmatrix} R_I \\ R_Q \end{pmatrix} = R \cdot \begin{pmatrix} S_I \\ S_Q \end{pmatrix} = \begin{bmatrix} \cos\theta & -\sin\theta \\ \sin\theta & \cos\theta \end{bmatrix} \cdot \begin{pmatrix} S_I \\ S_Q \end{pmatrix}, \tag{13}$$

where S_I/S_Q and R_I/R_Q represent the transmitted and the received in-phase and quadrature components of a single polarization complex signal, respectively. θ is the phase rotation degree induced by phase noise. For the complex expression of a constellation symbol, (13) can be simplified as

$$R_x = e^{j(\theta(t))} \cdot S_x, \tag{14}$$

where S_x and R_x denote the transmitted and the received single-polarization complex signal, respectively.

Therefore, after polarization-independent equalization, the received signals E_{mid} can be considered as the linear mixing of the transmitted signals S, which could be given as

$$E_{mid} = e^{j(\theta(t))} \cdot J(t) \cdot S = \begin{bmatrix} A(t)e^{j(\theta(t))} & B(t)e^{j(\theta(t))} \\ -B^*(t)e^{j(\theta(t))} & A^*(t)e^{j(\theta(t))} \end{bmatrix} \cdot S = M(t) \cdot S, \tag{15}$$

where $M(t)$ denotes a unitary 2×2 linearly mixed matrix. The impairments of RSOP and phase noise can be jointly compensated by estimating the inversely mixed matrix. Therefore, joint polarization de-multiplexing and phase recovery scheme can be expressed mathematically as

$$E_{out}(t) = \begin{bmatrix} w_{xx} & w_{xy} \\ w_{yx} & w_{yy} \end{bmatrix} \cdot E_{mid}(t) = W(t) \cdot E_{mid}(t), \tag{16}$$

where $W(t)$ is a 2×2 de-mixed matrix which should be also a unitary matrix.

As analyzed above, joint polarization de-multiplexing and phase recovery schemes exactly meet two requirements of blind source separation (BSS) technology [24]. The first requirement is that source signals are mutually independent, and the second requirement is that a mixed matrix is a square matrix. Based on the central limit theorem, the statistics of a mixed-signal tends to be more Gaussian than its independent source components [25]. Therefore, non-Gaussianity can measure the independence of signals. The BSS technology exactly extracts original independent source components by maximizing the non-Gaussianity of de-mixed signals [24]. NPCA is a kind of widely used BSS scheme based on high-order statistics (HOS) such as kurtosis, which can represent the non-Gaussianity of signals.

The output separation signals $E_{out}(t)$ are activated by a nonlinear function $g(\cdot)$ for taking HOS into accounts. According to the literation [18], the cost function of NPCA is expressed mathematically as

$$\mathbf{J}(W) = E\left\{\left|e(t)\right|^2\right\} = E\left\{\left|E_{mid}(t) - W^H \cdot g(E_{out}(t))\right|^2\right\}, \tag{17}$$

where $e(t)$ denotes the error. The nonlinear active function in NPCA is chosen to $g(\cdot) = tanh(\cdot)$ for the sub-Gaussian source signal. The cost function in (17) is equivalent to the kurtosis of the recovered signal [26], which represents the non-Gaussianity of the output separated signals. To separate not only two independent polarization complex signals but also independent in-phase and quadrature components in single-polarization complex signals, nonlinear active function for the complex value is always expressed as the combination of the real part $g(real(E_{out}))$ and imaginary part $g(imag(E_{out}))$, and it is given as $g(E_{out}) = g(real(E_{out})) + g(imag(E_{out}))$.

Generally, an adaptive iterative algorithm like the LMS method is required to minimize the cost function J(W). A common parameter update method based on LMS-NPCA is mathematically given as

$$W(t) = W(t-1) + \mu \cdot \left[e^*(t) \cdot g^T(E_{out}(t-1))\right]^T, \tag{18}$$

where the superscript $*$ and T denotes the complex conjugate and transpose operation, respectively. LMS-NPCA is based on stochastic gradient descent optimization which is sensitive to the step size. Usually, a small step size could help achieve minimization of steady-state mean square

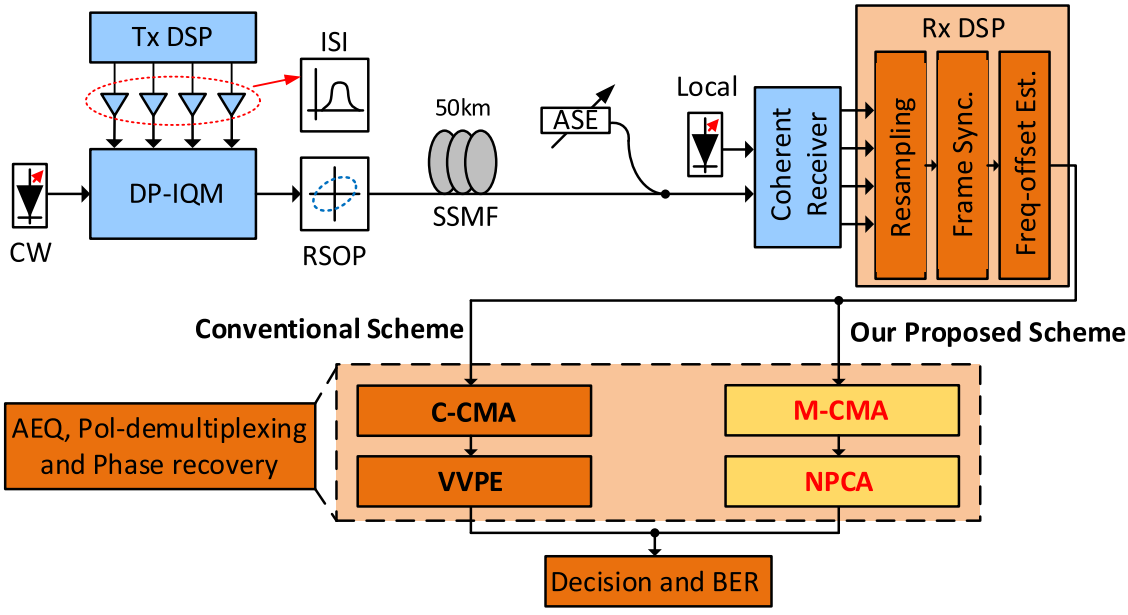

Fig. 4. The simulation setup of the PDM-QPSK coherent optical system and DSP flow.

error (MSE), but it will lead to poor convergence rate and slow tracking speed. For dynamic channel conditions such as ultra-fast RSOP and time-varying phase noises, we consider an RLS minimization method for NPCA. RLS methods converge faster, and they have better final accuracy than stochastic gradient descent algorithms [27]. Therefore, the cost function in (17) can be modified as

$$\mathbf{J}(W) = \sum_{i=1}^{t} \lambda^{t-i} \cdot \left\| e(t) \right\|^2 = \sum_{i=1}^{t} \lambda^{t-i} \cdot \left\| E_{mid}(t) - W^H \cdot g(E_{out}(t)) \right\|^2, \tag{19}$$

where λ is the tuning forgetting factor. If $\lambda = 1$, all the samples are given the same weight, and no forgetting of old data takes place. Generally, $\lambda < 1$ is useful in tracking nonstationary changes. The de-mixed matrix W is updated by RLS-NPCA as

$$h(t) = P(t-1) \cdot g(E_{out}(t)), \tag{20}$$

$$K(t) = h(t)/(\lambda + g(E_{out}(t))^H \cdot h(t)), \tag{21}$$

$$P(t) = 1/\lambda \cdot Tri\left[P(t-1) - K(t) \cdot h^H(t)\right], \tag{22}$$

$$W(t) = W(t-1) + K(t) \cdot e^H(t), \tag{23}$$

where P is a Hermite matrix initializing to a unit matrix. *Tri* means that only the upper triangular part of the argument is computed and its transpose-conjugate is copied to the lower triangular part. Because $W(t)$ is a matrix with a small dimension of 2×2, the computational complexity of RLS-NPCA is a little higher than that of LMS-NPCA.

3. Simulation Setup and Results

To verify the feasibility of the proposed algorithm, a simulation system using MATLAB and VPI-transmissionMaker 9.0 is built up as shown in Fig. 4. Two sets of independent pseudorandom bit sequences (PRBS) with a length of 56000 are produced and then mapped into 28 GBaud PDM-QPSK symbols. These symbols are resampled at the twice sampling rate and pulse-shaped

using a square root raised cosine FIR filter whose roll-off factor is 0.2. A continuous-wave (CW) light with a linewidth of 100 kHz is used as the optical source. Four path mutually independent signals are used to drive an optical dual-polarization I/Q modulator (DP-IQM). Besides, a bandwidth-limited filter to emulate the ISI effect, an RSOP emulator, a 50 km SSMF are all considered in the transmission link. Dynamic RSOP in our test can be described using the Jones matrix as $[\cos\omega t \cdot e^{j\xi}, -\sin\omega t \cdot e^{j\eta}; \sin\omega t \cdot e^{-j\eta}, \cos\omega t \cdot e^{-j\xi}]$ [23], here ξ and η correspond to phase angles, and ω denotes the speed of the polarization rotation. It should be noted that the dispersion parameter of the fiber is set to 16 ps/(nm·km), PMD is set to 0.1 ps/km$^{1/2}$, and fiber loss is set to 0.2 dB/km. ASE noise is introduced into the signal to adjust the optical signal-to-noise ratio (OSNR). In the receiver, another laser with a linewidth of 100 kHz is used as the local oscillator. The received signals are captured by the coherent receiver. In the receiver DSP module, the received signals are first resampled and synchronized, and then frequency offset is estimated by the algorithm of maximum fast Fourier transform. Finally, our proposed scheme (M-CMA+NPCA) and the conventional scheme (C-CMA+VVPE) are both used for equalization, polarization de-multiplexing, and phase recovery.

The OSNR value of the optical signal at the receiver is set to 13 dB. A 3 dB bandwidth of 10 GHz filter is used to emulate the ISI effect from nonideal devices. A fixed static RSOP with rotation degree of $\pi/3$ is used in our test. For dynamic RSOP simulation, an RSOP of 1 Mrad/s emulator is used. The tap number and step size of FIR filters based on M-CMA are set to 29 and 0.001, respectively. The step size of LMS-NPCA is set to 0.1, and the forgetting factor of RLS-NPCA is set to 0.85. Fig. 5(a)–(d) illustrates transformations of signal constellation diagram using M-CMA for ISI equalization and NPCA for polarization and phase tracking. Fig. 5(a) shows the constellation diagrams of two polarization coupling signals without any compensation. Based on the fact that the power sum of two orthogonal polarization optical signals remains constant, M-CMA is employed to equalize polarization coupling signals. The constellation diagrams of two polarization coupling signals are shown in Fig. 5(b), and they get relatively converged. That means these two signals are still impaired by RSOP and phase noise. Subsequently, NPCA is used for signal recovery as shown in Fig. 5(c). The electrical spectrum of the received signal without any equalizer is plotted in Fig. 5(d), and the high-frequency components are suppressed on account of ISI. After M-CMA whose error amplitude convergence diagram is illustrated in Fig. 5(e), the electrical spectrum of the signal becomes flat as shown in Fig. 5(f).

NPCA is used to separate two independent polarization complex signals for polarization de-multiplexing and independent I/Q real signals for phase recovery. The convergence diagrams of coefficients in the de-mixed matrix of LMS-NPCA and RLS-NPCA are showed in Fig. 6(a)–(d). The estimated de-mixed matrix $W(t)$ is described as $[w_{xx}, w_{xy}; w_{yx}, w_{yy}]$, and each coefficient is a complex value. The modulus of the complex values represent the polarization demultiplexing coefficient, and the angle of the complex values represent the phase tacking angle. In the simulation, $\text{abs}(w_{xx})$, $\text{abs}(w_{xy})$ are selected as illustrations to plot polarization demultiplexing coefficient convergence diagram of LMS-NPCA and RLS-NPCA as shown in Fig. 6(a) and 6(b), respectively. And $\text{angle}(w_{xx})$ is selected as an illustration to plot the phase tacking fluctuation diagram of LMS-NPCA and RLS-NPCA as shown in Fig. 6(c) and 6(d), respectively. It can be seen that the polarization demultiplexing coefficient is slowly varying due to the RSOP of 1 Mrad/s. These two NPCA schemes both have quick convergence at the earlier stage, and RLS-NPCA has a litter faster convergence speed than LMS-NPCA. Overall, these two schemes can both track the polarization state changes and phase fluctuations very well.

The dynamic RSOP tracking ability on the proposed schemes and the conventional scheme is evaluated in our test, and the OSNR value of the received optical signal is fixed at 13 dB. The used dynamic RSOP model can be described using the Jones transformation matrix $[\cos\omega t \cdot e^{j\xi}, -\sin\omega t \cdot e^{j\eta}; \sin\omega t \cdot e^{-j\eta}, \cos\omega t \cdot e^{-j\xi}]$ [23], here ω denotes the angular speed of polarization rotation. Fig. 7(a) illustrates the measured BER performance of 112 Gb/s PDM-QPSK signal after 50 km SSMF transmission in terms of dynamic RSOP with different rotation speeds, and the conventional C-CMA+VVPE and the proposed schemes based on M-CMA+LMS /RLS-NPCA are all tested and compared. The tap number and step size of FIR filters based on C-CMA are also

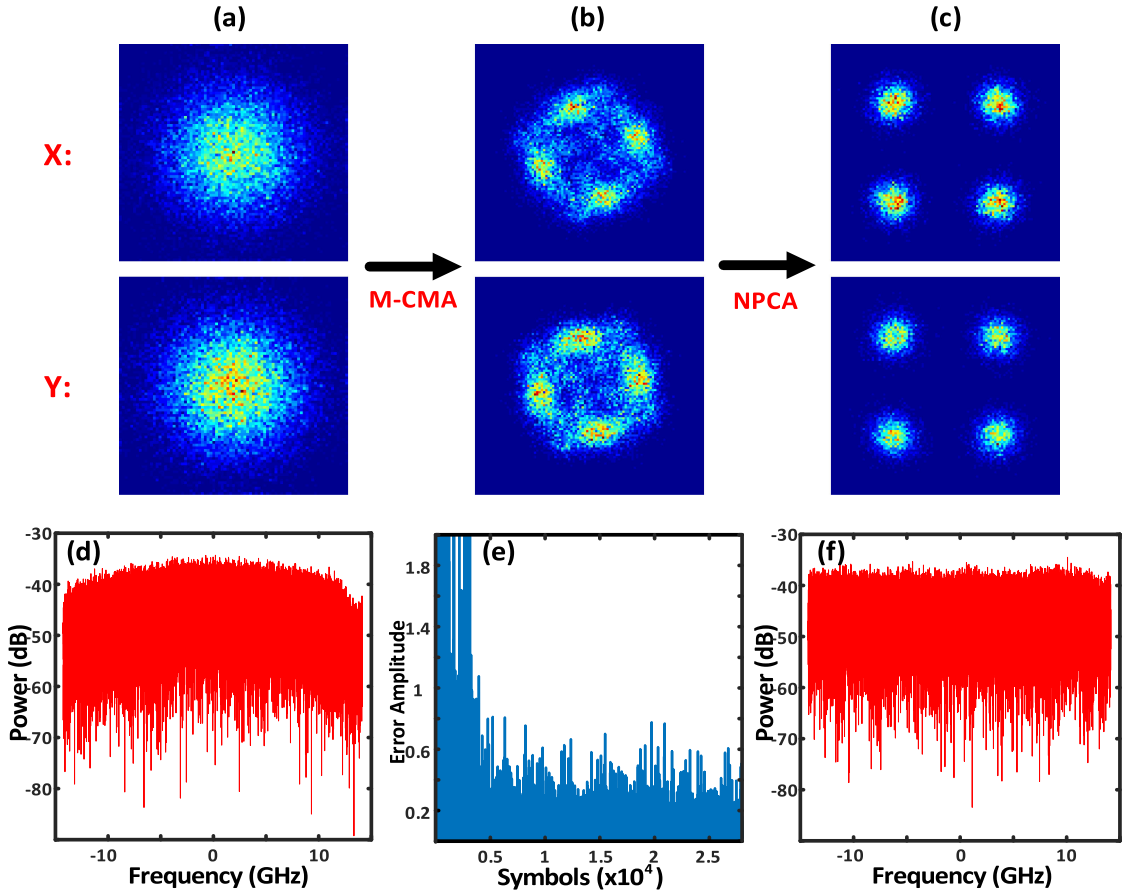

Fig. 5. QPSK constellation diagram before M-CMA+NPCA (a), after M-CMA (b), after NPCA (c). The electrical spectrum of the signal without any equalizer (d). The error amplitude convergence diagram of M-CMA (e). The electrical spectrum of the signal with M-CMA (f).

set to 29 and 0.001 [28]. It can be seen that only RSOP of $<$1 Mrad/s can be tracked using the conventional C-CMA+VVPE algorithm. RSOP of 10 Mrad/s could still be tracked by using the proposed two schemes. It is reported that the polarization rotation speed of SOP will be as fast as 5.4 Mrad/s in [5], and that means the proposed schemes can perfectly overcome this problem. And owing to faster convergence speed, it can be also seen that the polarization tracking speed of the RLS-NPCA is a little faster than that of the LMS-NPCA.

The phase recovery ability of LMS-NPCA, RLS-NPCA, and VVPE is also tested. In our test, the OSNR value of the optical signal at the receiver is fixed at 13 dB, and static RSOP is considered. Fig. 7(b) shows the measured BER performance of 112 Gb/s PDM-QPSK signal after OBTB transmission in terms of different laser linewidth. The conventional VVPE, the LMS-NPCA with different step size μ, and the RLS-NPCA with different forgetting factor λ are tested and compared. Noted that in the VVPE scheme, the phase shift of signals is estimated by averaging a block of adjacent signals with the length of N, and N is set to 40 in our test. NPCA scheme can adaptively update the de-mixed matrix of phase noises to recover phases of signals, and the step size in the LMS-NPCA and the forgetting factor in the RLS-NPCA will influence the convergence and tacking speed. It could be observed in Fig. 7(b) that the larger step size in the LMS-NPCA and the smaller forgetting factor in the RLS-NPCA could both contribute to higher laser linewidth tolerance and relatively bad BER performance in the condition of narrow laser linewidth. This could be attributed to the fact that NPCA is a gradient descent optimization algorithm. The bigger the step size of

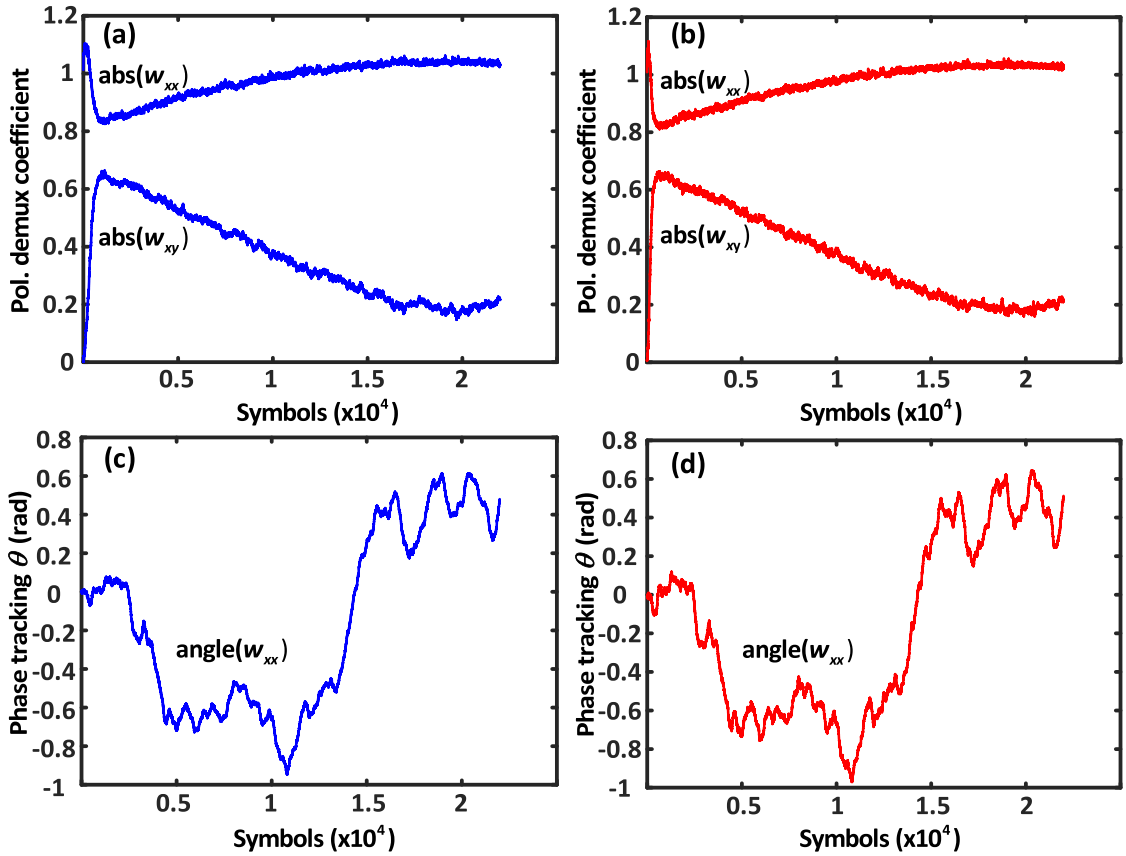

Fig. 6. Polarization demultiplexing coefficient convergence and tracking diagram using LMS-NPCA (a), and RLS-NPCA (b). Phase tacking fluctuations diagram using LMS-NPCA (c), and RLS-NPCA (d).

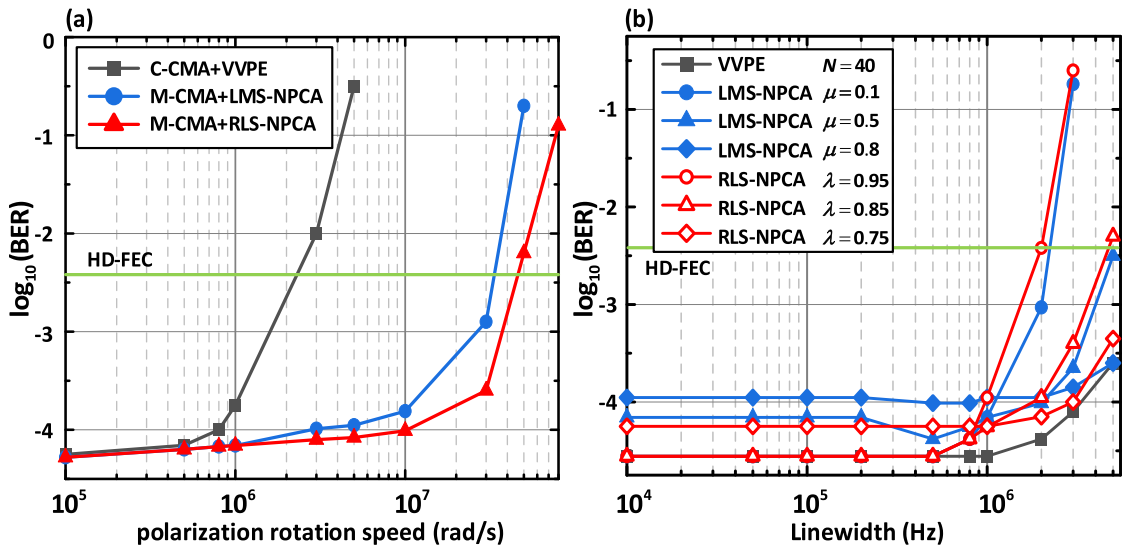

Fig. 7. The measured BER performance in terms of polarization rotation speed (a) and laser linewidth (b) using different equalizers.

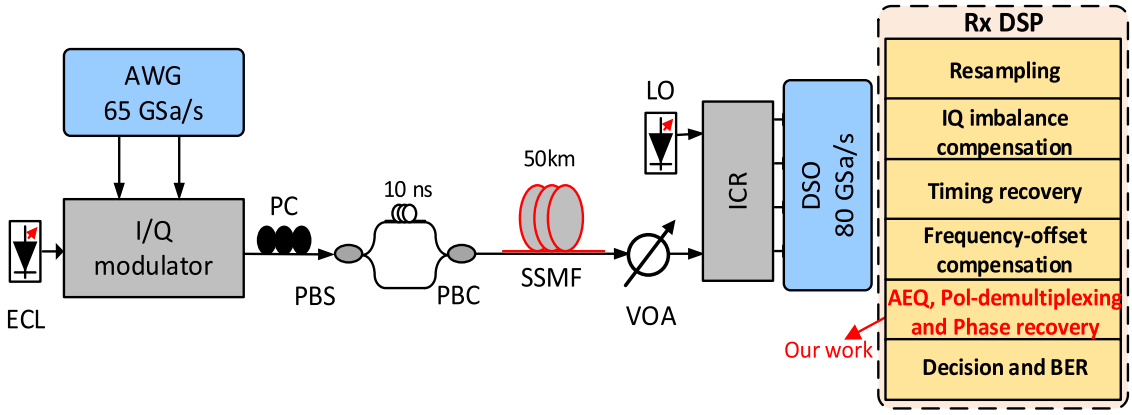

Fig. 8. The experimental setup of 112 Gb/s PDM-QPSK coherent optical transmission system using the proposed schemes.

the LMS-NPCA or the smaller the forgetting factor of the RLS-NPCA, the faster the convergence and dynamic tracking. Unfortunately, the additive white Gaussian noise will have a big impact on the proposed algorithm when the step size is large and the forgetting factor is small, especially in the condition of narrow laser linewidth. Therefore, in consideration of both BER performance and laser linewidth tolerance, the LMS-NPCA with the step size of 0.1 and the RLS-NPCA with the forgetting factor of 0.85 is selected for the following experiment. However, the phase recovery ability of NPCA and VVPE is similar when the laser linewidth is less than 1 MHz, and thus no additional phase recovery module is required in NPCA. Compared to the traditional C-CMA+VVPE scheme, the proposed M-CMA+NPCA schemes have better RSOP tracking ability and lower computation complexity.

4. Experimental Setup and Results

Fig. 8 shows the experimental setup of 112 Gb/s PDM-QPSK signal transmission over 50 km SSMF. At the transmitter, the transmitting 56000 symbols are generated offline with MATLAB. These symbols are pulse-shaped by a square root raised cosine FIR filter whose roll-off factor is 0.2 and then loaded into an arbitrary waveform generator (AWG, Keysight M8195A) operating at 65 GSa/s. An external cavity laser (ECL) with a linewidth of 100 kHz and a wavelength of 1550.12 nm is used as the optical source. The electrical signals are used to drive an optical I/Q modulator (Fujitsu, FTM7961EX). To implement the polarization division multiplexing, the modulated optical signal is divided into two orthogonal signals by a polarization controller (PC) and a polarization beam splitter (PBS). One of the optical signals is delayed by 10 ns for decorrelation, and then two polarization state optical signals are combined by a polarization beam combiner (PBC). The optical power of transmitted PDM-QPSK signals is about -12.5 dBm. After 50 km SSMF propagation without any optical amplifier, the received optical power (ROP) is controlled by a variable optical attenuator (VOA). Finally, the received optical signal is beat with the local oscillator (LO) light with a linewidth of 100 kHz and a wavelength of 1550.12nm in an integrated coherent receiver (ICR, Fujitsu, FIM24706/301), and the optical power of LO light is set to 10 dBm. The detected electrical signals are captured by a digital sampling oscilloscope (DSO, LeCroy LabMaster 10-36Zi-A) at 80 GSa/s for the offline process. Finally, the DSP modules are employed to compensate for the impairments. To be specific, Gram-Schmidt orthogonalization produce (GSOP) is used for eliminating the IQ imbalance. The timing error is compensated by the Godard algorithm and the frequency offset is estimated by the algorithm of maximum fast Fourier transform. Then our proposed M-CMA+NPCA schemes and the conventional C-CMA+VVPE scheme are both

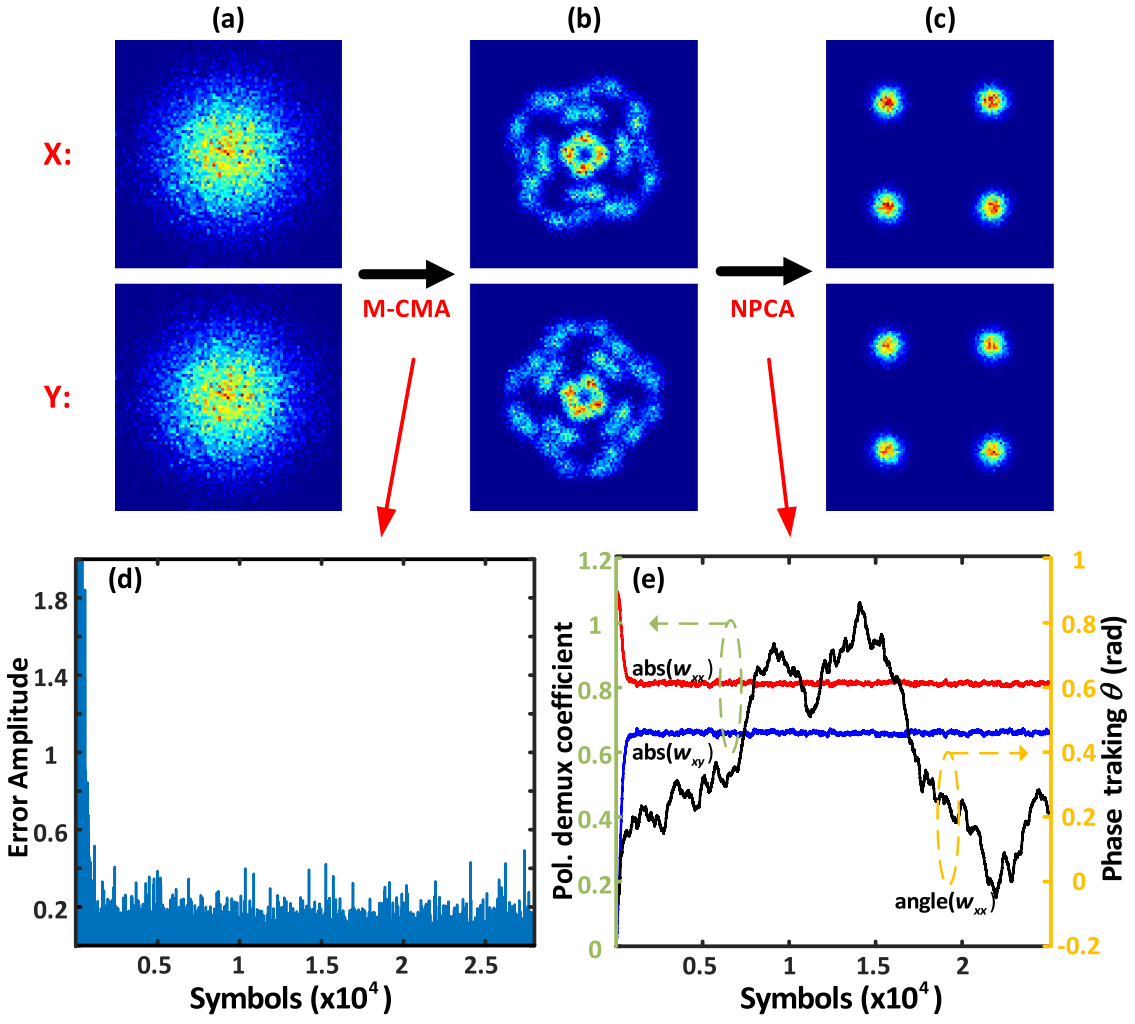

Fig. 9. The received signal constellation diagram without M-CMA+NPCA (a), after M-CMA (b) and NPCA (c). The error amplitude convergence curve of M-CMA (d). The convergence curve of the de-mixed matrix coefficient and the tracked phase fluctuations using LMS-NPCA (e).

used for equalization, polarization de-multiplexing, and phase recovery. Finally, QPSK symbols are demodulated and BER performance is evaluated.

Fig. 9 shows the constellation diagram transformations of the received signal using the proposed M-CMA+NPCA scheme when ROP is −23 dBm. In this test, two one-dimensional 29 taps FIR filters based on M-CMA are used to equalize the ISI effect. With the help of M-CMA, the badly dispersive signal constellation diagram shown in Fig. 9(a) becomes relatively converged shown in Fig. 9(b). It's worth noting that the signal shown in Fig. 9(b) is also impaired by polarization coupling and phase noise. Therefore, NPCA is then used for polarization de-multiplexing and phase recovery, and the recovered signal constellation diagram is plotted in Fig. 9(c). Fig. 9(d) presents the error amplitude convergence curve of M-CMA. For the conciseness of the plotting diagram, Fig. 9(e) shows the convergence curve of the de-mixed matrix coefficient and the tracked phase fluctuations using LMS-NPCA. It can be seen that LMS-NPCA has quick convergence and dynamic tracking ability for simultaneously polarization state and phase tracking.

Fig. 10(a) shows the measured BER performances of 112 Gb/s PDM-QPSK signals as a function of ROP after 50 km SSMF transmission using different equalizers. It can be seen that the proposed schemes (M-CMA+LMS-NPCA and M-CMA+RLS-NPCA) and the conventional C-CMA+VVPE

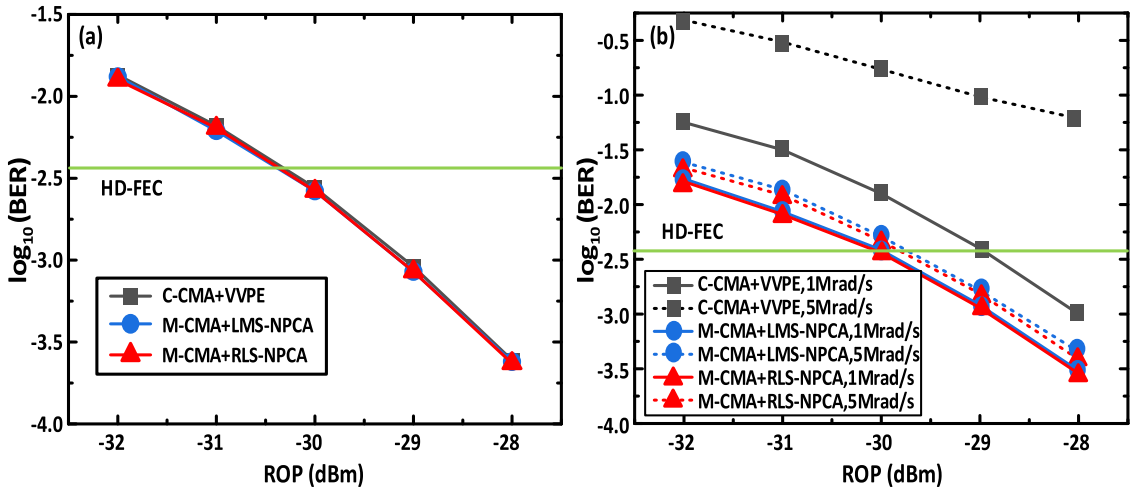

Fig. 10. The measured BER performance of 112 Gb/s PDM-QPSK signals after 50 km SSMF transmission at the static RSOP scenario (a), and the dynamic RSOP of 1 Mrad/s and 5 Mrad/s scenarios (b).

TABLE 1
The Computational Complexity of These Three Equalization Schemes (per Symbol)

Algorithm	Number of multiplications	value
C-CMA+VVPE	32N+38	966
M-CMA+LMS-NPCA	16N+66	530
M-CMA+RLS-NPCA	16N+102	566

scheme have similar transmission performance, and the achieved receiver sensitivity at the hard-decision forward error correction (HD-FEC) threshold of 3.8×10^{-3} is -30.4 dBm in each case. This could be attributed to the fact that the RSOP is static under laboratory conditions, and the conventional scheme is good enough for tracking this slow RSOP. To analyze the dynamic polarization tracking ability of the proposed schemes, the endless polarization rotation is digitally achieved by a polarization rotation Jones transformation matrix in the receiver DSP module before the polarization demultiplexing [23]. In this test, the RSOP speed is set to 1 Mrad/s and 5 Mrad/s for polarization tracking performance comparison. Fig. 10(b) presents the measured BER performance of 112 Gb/s PDM-QPSK signals as a function of ROP after 50 km SSMF transmission in the dynamic RSOP scenarios. When the RSOP of 1 Mrad/s is used, the proposed two schemes both outperform the conventional C-CMA+VVPE scheme, and about 1 dB power penalty at the HD-FEC is observed. When the RSOP speed is increased to 5 Mrad/s, the transmission performance deteriorates severely in the conventional C-CMA+VVPE scheme, which is consistent with the simulation results in Fig. 7(a). The proposed two schemes show strong RSOP tolerance, and negligible power penalty is observed compared to the RSOP of 1 Mrad/s. However, the proposed M-CMA+RLS-NPCA scheme has a little better transmission performance than the proposed M-CMA+LMS-NPCA at the cost of complexity. Therefore, it has been proven that the proposed schemes could achieve a fast polarization state and phase tracking with lower complexity, compared to the traditional C-CMA+VVPE scheme.

5. Complexity Analysis and Comparison

The computational complexity of the proposed M-CMA+NPCA schemes and the conventional C-CMA+VVPE scheme are compared as shown in Table 1. Note that the computational complexity is analyzed based on the principle that a product between two complex value needs 4 real

multipliers and 2 real adders, and a product between a real value and a complex value needs 2 real multipliers. Moreover, methods of look-up tables are adopted to calculate the complexity of nonlinear function and phase noise angle. In our test, the computational complexity can be calculated in terms of the required number of the real-valued multiplications per symbol, because the cost of a multiplier is higher than that of an adder and look-up table.

In the conventional C-CMA+VVPE scheme, there are 4N complex-valued multiplications in the equalization process, 2 complex-valued multiplications in error calculation, and 4N complex-valued and 6 real-valued multiplications in the feedback updating process. Besides, there are 6 complex-valued multiplications for two polarization signals in VVPE. Therefore, 32N+38 equivalent real multipliers are required for the conventional CMA+VVPE algorithm. In the proposed schemes, two modified CMA filters need 4N complex-valued multiplications for equalization, 2 complex-valued multiplications for error calculating, and 2N complex-valued and 6 real-valued multiplications for feedback updating processing. Besides, the LMS-NPCA and RLS-NPCA algorithm need 52 and 88 real-valued multiplications, respectively. Therefore, there are 16N+66 and 16N+102 equivalent real multipliers in the proposed M-CMA+LMS-NPCA algorithm and M-CMA+RLS-NPCA algorithm, respectively. As shown in Table 1, the FIR filter length is N. In our test, N is set to 29 in both static and dynamic RSOP scenarios. Therefore, 966 real multipliers are needed for the conventional CMA+VVPE scheme. Just 530 and 566 real multipliers are respectively required in the proposed M-CMA+LMS-NPCA and M-CMA+RLS-NPCA scheme, and the complexity reduction is about 45% and 41%, respectively.

6. Conclusion

A low-complexity joint adaptive equalization, polarization de-multiplexing, and phase recovery scheme for PDM-QPSK optical transmission system is proposed and experimentally demonstrated. The proposed scheme has two one-dimensional N-tap filters for polarization-independent dispersion equalization based on M-CMA, and a 1-tap 2 $\times$ 2 filter for polarization de-multiplexing and phase recovery based on NPCA. In our simulation, NPCA is proved to realize phase recovery even when the laser linewidth is 4 MHz. When static RSOP scenario is considered, compared to the conventional C-CMA+VVPE scheme, the proposed M-CMA+NPCA schemes show similar BER performance in an experiment of 112 Gb/s PDM-QPSK signal transmission over 50 km SSMF. When the RSOP speed is increased to 5 Mrad/s, the transmission performance deteriorates severely in the conventional C-CMA+VVPE scheme, but the proposed two schemes show strong RSOP tolerance. Moreover, the proposed two schemes have lower complexity, and the complexity reduction is more than 40%. These results predict that the proposed DSP scheme may have a promising prospect for cost-effective coherent optical transmission systems.

References

[1] X. Li *et al.*, "Transmission of 4 $\times$ 28-Gb/s PAM-4 over 1 references 60-km single mode fiber using 10G-class DML and photodiode," in *Proc. Opt. Fiber Commun. Conf.*, 2016, Paper W1A.5.
[2] S. Zhou, X. Li, L. Yi, Q. Yang, and S. Fu, "Transmission of 2x56Gb/s PAM-4 signal over 100 km SSMF using 18 GHz DMLs," *Opt. Lett.*, vol. 41, no. 8, pp. 1805–1808, Apr. 2016.
[3] J. Zhang *et al.*, "Demonstration of 260-Gb/s single-lane EML-based PS-PAM-8 IM/DD for datacenter interconnects," in *Proc. Opt. Fiber Commun. Conf.*, 2018, Paper W4E.1.
[4] M. Osman *et al.*, "A comparative study of next generation intra- and inter-datacenter interconnects," in *Proc. Opt. Fiber Commun. Conf.*, 2019, Paper W4I.4.
[5] D. Charlton *et al.*, "Field measurements of SOP transients in OPGW, with time and location correlation to lightning strikes," *Opt. Exp.*, vol. 25, no. 9, pp. 9689–9696, May 2017.
[6] M. Kuscherov and M. Herrmann, "Lightning affects coherent optical transmission in aerial fiber," *Lightwave*, 2016, [Online]. Available: https://www.lightwaveonline.com/articles/2016/03/lightning-affects-coherent-optical-transmission-inaerial-fiber.html
[7] D. A. Morero *et al.*, "Design trade-offs and challenges in practical coherent optical transceiver implementations," *J. Lightw. Technol.*, vol. 34, no. 1, pp. 121–136, Jan. 2016.
[8] R. Corsini *et al.*, "Blind adaptive chromatic dispersion compensation and estimation for DSP-based coherent optical systems," *J. Lightw. Technol.*, vol. 31, no. 13, pp. 2131–2139, Jul. 2013.

[9] M. Saifuddin Faruk and K. Kikuchi, "Adaptive frequency-domain equalization in digital coherent optical receivers," *Opt. Exp.*, vol. 19, no. 13, pp. 12789–12798, Jul. 2011.
[10] M. Morsy-Osman *et al.*, "Ultrafast and low overhead training symbol based channel estimation in coherent M-QAM single-carrier transmission systems," *Opt. Exp.*, vol. 20, no. 26, pp. B171–B180, Dec. 2012.
[11] K. Matsuda, R. Matsumoto, and N. Suzuki, "Hardware-efficient adaptive equalization and carrier phase recovery for -based coherent WDM-PON systems," *J. Lightw. Technol.*, vol. 36, no. 8, pp. 1492–1497, Apr. 2018.
[12] X. Zhang *et al.*, "Real time low-complexity adaptive channel equalization for coherent optical transmission systems," *Opt. Exp.*, vol. 28, no. 4, pp. 5058–5068, Feb. 2020.
[13] T. Zeng *et al.*, "The real time implementation of a simplified 2-section equalizer with supernal SOP tracking capability," in *Proc. Opt. Fiber Commun. Conf.*, 2020, Paper M2J.7.
[14] K. Kikuchi, "Performance analysis of polarization demultiplexing based on constant-modulus algorithm in digital coherent optical receivers," *Opt. Exp.*, vol. 19, no. 10, pp. 9868–9880, May 2011.
[15] P. M. Krummrich *et al.*, "Demanding response time requirements on coherent receivers due to fast polarization rotations caused by lightning events," *Opt. Exp.*, vol. 24, no. 11, pp. 12442–12457, May 2016.
[16] Y. Yang *et al.*, "Fast polarization-state tracking scheme based on radius-directed linear Kalman filter," *Opt. Exp.*, vol. 23, no. 15, pp. 19673–19680, Jul. 2015.
[17] Q. Zhang *et al.*, "Modulation-format-transparent IQ imbalance estimation of dual-polarization optical transmitter based on maximum likelihood independent component analysis," *Opt. Exp.*, vol. 27, no. 13, pp. 18055–18068, Jun. 2019.
[18] Q. Xiang, Y. Yang, Q. Zhang, and Y. Yao, "Low complexity, modulation-transparent and joint polarization and phase tracking scheme based on the nonlinear principal component analysis," *Opt. Exp.*, vol. 27, no. 13, pp. 17968–17977, Jun. 2019.
[19] Q. Xiang, Y. Yang, Q. Zhang, and Y. Yao, "Fast and format-transparent polarization tracking scheme based on nonlinear principal component analysis criterion," in *Proc. Opt. Fiber Commun. Conf.*, 2019, Paper W2A.52.
[20] A. J. Viterbi and A. M. Viterbi, "Nonlinear estimation of PSK-modulated carrier phase with application to burst digital transmission," *IEEE Trans. Inf. Theory*, vol. 29, no. 4, pp. 543–551, Jul. 1983.
[21] T. Pfau, S. Hoffmann, and R. Noe, "Hardware-efficient coherent digital receiver concept with feedforward carrier recovery for M-QAM constellations," *J. Lightw. Technol.*, vol. 27, no. 8, pp. 989–999, Apr. 2009.
[22] Z. Zheng *et al.*, "Window-split structured frequency domain kalman equalization scheme for large PMD and ultra-fast RSOP in an optical coherent PDM-QPSK system," *Opt. Exp.*, vol. 26, no. 6, pp. 7211–7226, Mar. 2018.
[23] N. Cui *et al.*, "Two-parameter-SOP and three-parameter-RSOP fiber channels: Problem and solution for polarization demultiplexing using stokes space," *Opt. Exp.*, vol. 26, no. 16, pp. 21170–21183, Aug. 2018.
[24] P. Comon, "Independent component analysis, a new concept?," *Signal Process.*, vol. 36, pp. 287–314, Aug. 1994.
[25] R. Murray, "A central limit theorem and a strong mixing condition," *Proc. Nat. Acad. Sci. United States America*, vol. 42, no. 1, pp. 43–47, 1956.
[26] M. Girolami and C. Fyfe, "Stochastic ICA contrast maximization using OJA's nonlinear PCA algorithm," *Int. J. Neural Syst.*, vol. 8, no. 5-6, pp. 661–678, Jun. 1997.
[27] E. Oja, "The nonlinear PCA learning rule and signal separation-mathematical analysis," Helsinki Univ. of Tech., Lab. Comput. Inf. Sci., Finland, Rep. A26, Aug. 1995.
[28] W. Yi *et al.*, "Joint equalization scheme of ultra-fast RSOP and large PMD compensation in presence of residual chromatic dispersion," *Opt. Exp.*, vol. 27, no. 15, pp. 21896–21913, Jul. 2019.